Confinement modeling of enhanced plasma performance after multiple pellet injections in the TJ-II stellarator

V. Tribaldos[1], I. García-Cortés[2], K.J. McCarthy[2], J.M. Reynolds-Barredo[1], B. van Milligen[2], A. Baciero[2], J. de la Riva[2], J.L. de Pablos[2], O.S. Kozachek[3], I. Pastor[2] and the TJ-II TEAM

[1]*Departmento de Física, Universidad Carlos III de Madrid, Leganés, Spain*

[2]*Laboratorio Nacional de Fusión, Ciemat, Madrid, Spain*

[3]*Institute of Plasma Physics, NSC KIPT Kharkiv, Ukraine*

Introduction

Recent experimental campaigns on the TJ-II stellarator have investigated the effects of multiple cryogenic hydrogen pellet injections into neutral beam injection (NBI)-heated plasmas [1, 2]. The plasmas generated through multiple pellet injections exhibit sustained record central densities, ion temperatures, and normalized β. Compared to standard gas-puffing, the deep plasma fueling provided by multi-pellet injection leads to sharp increases in line-averaged density $\langle n_e \rangle$ and diamagnetic energy W. Thomson scattering profiles reveal broader, dense core profiles with only minor changes in the electron temperature. This aligns with the expected electron-to-ion collisional energy transfer ($Q_{ei} \propto n_e^2(T_e - T_i)/T_e^{3/2}$), which slightly cools electrons while significantly heating ions. Charge-exchange recombination spectroscopy (CXRS) confirms broader T_i profiles with notably higher central values, pointing toward a modification in ion transport. While a significant decrease in density and electrostatic potential fluctuations in the outer plasma region indicates a clear turbulent transport contribution [3], the more negative values of the radial electric field, measured with a Heavy Ion Beam Probe (HIBP) and CXRS, also point toward a neoclassical transport mechanism induced by pellet injection. This neoclassical component will be further explored in the following section.

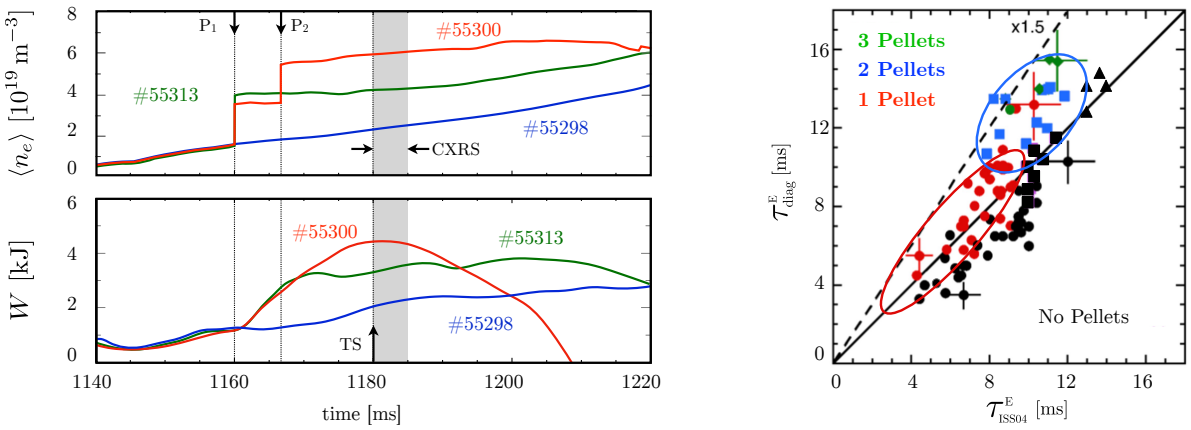

Figure 1: *Left: Line-averaged density and stored diamagnetic energy traces without pellets #55298, with one pellet #55313, and with two pellets #55300. Right: Energy confinement time vs. ISS04 scaling.*

Neoclassical Simulations

To isolate the neoclassical transport contribution, local simulations were performed across three distinct discharges, see Figures 1 and 2: a gas-puffing reference #55298, a single-pellet discharge #55313, and a two-pellet discharge #55300. Local particle fluxes $\Gamma_\alpha(E_r)$, energy fluxes $Q_\alpha(E_r)$, and bootstrap current densities $J^b_\alpha(E_r)$ are evaluated from the density and temperature profiles for all species α using the monoenergetic drift-kinetic approach [4, 5]. The three required monoenergetic diffusion coefficients D_{11} for particle transport, D_{31} for bootstrap, and D_{33} for conductivity are computed using the MOCA [6] and DKES [7] codes for the standard 100_44_64 magnetic configuration. Parallel momentum conservation was satisfied using the correction technique described in [8]. The simulation inputs and calculated profiles, see Figure 3, show clear, consistent trends across the pellet sequence.

For the reference gas-puff discharge #55298, the ions reside at the boundary of the highly collisional Pfirsch-Schlüter regime. Following multiple pellet injections, the increased ion temperature pushes the core ion population fully into the plateau regime for discharges #55313 and #55300. In all analyzed cases, electrons remain fixed in the plateau regime.

Because neoclassical fluxes drop significantly at the cold, highly collisional plasma edge, core neoclassical estimates are obtained around the gradient zone ($r/a \approx 2/3$). For the reference discharge ($W = 2.4$ kJ), the surface-integrated neoclassical power losses account for ~ 50 kW, rising to ~ 100 kW in the two-pellet case ($W = 4.4$ kJ), as shown in Figure 3. For $P_{\mathrm{NBI}} = 320$ kW, this indicates that the neoclassical transport channel accounts for only about one third of the total energy transport. Moreover, as summarized in Table 1, the experimental energy confinement time τ_E^{exp} systematically improves across the discharges, whereas τ_E^{NC} remains almost constant. This invariant behavior occurs

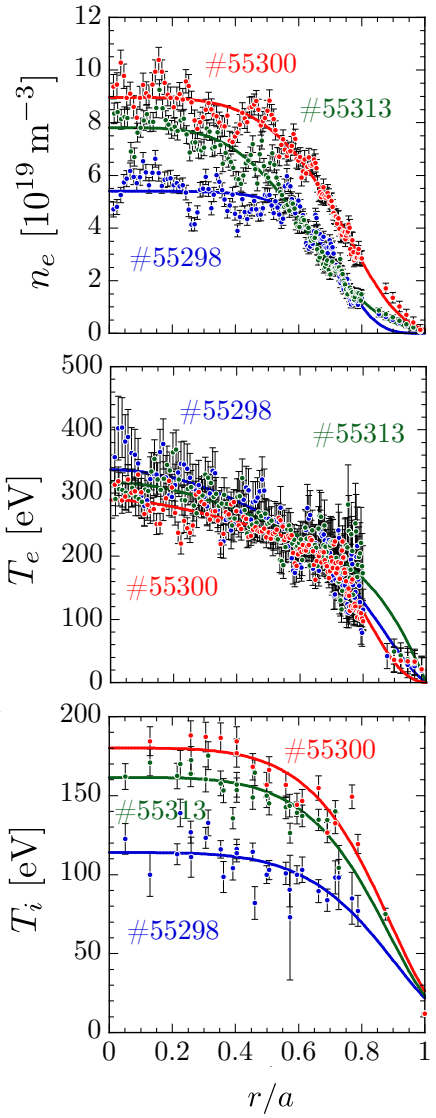

Figure 2: *Plasma profiles without pellets (#55298), with one pellet (#55313), and with two pellets (#55300) from TS and CXRS of Fig. 1.*

because both the stored energy W and the neoclassical power losses P_{NC} scale proportionally. Consequently, the simulated confinement time remains roughly constant. The weak dependence identified by the model is entirely consistent with the physics of the transition from the Pfirsch-Schlüter to the plateau regime. Nevertheless, the neoclassical simulations provide other physical quantities that can be cross-checked against experimental data, namely, the radial electric field and the bootstrap current. For these discharges, the ambipolar radial electric field E_r^*, obtained by solving the ambipolarity condition $\sum_\alpha Z_\alpha \Gamma_\alpha(E_r^*) = 0$, becomes systematically more negative in the gradient region ($r/a \sim 0.8$) for multi-pellet discharges, reaching values between -5 and -10 kV/m, in agreement with HIBP and CXRS experimental measurements.

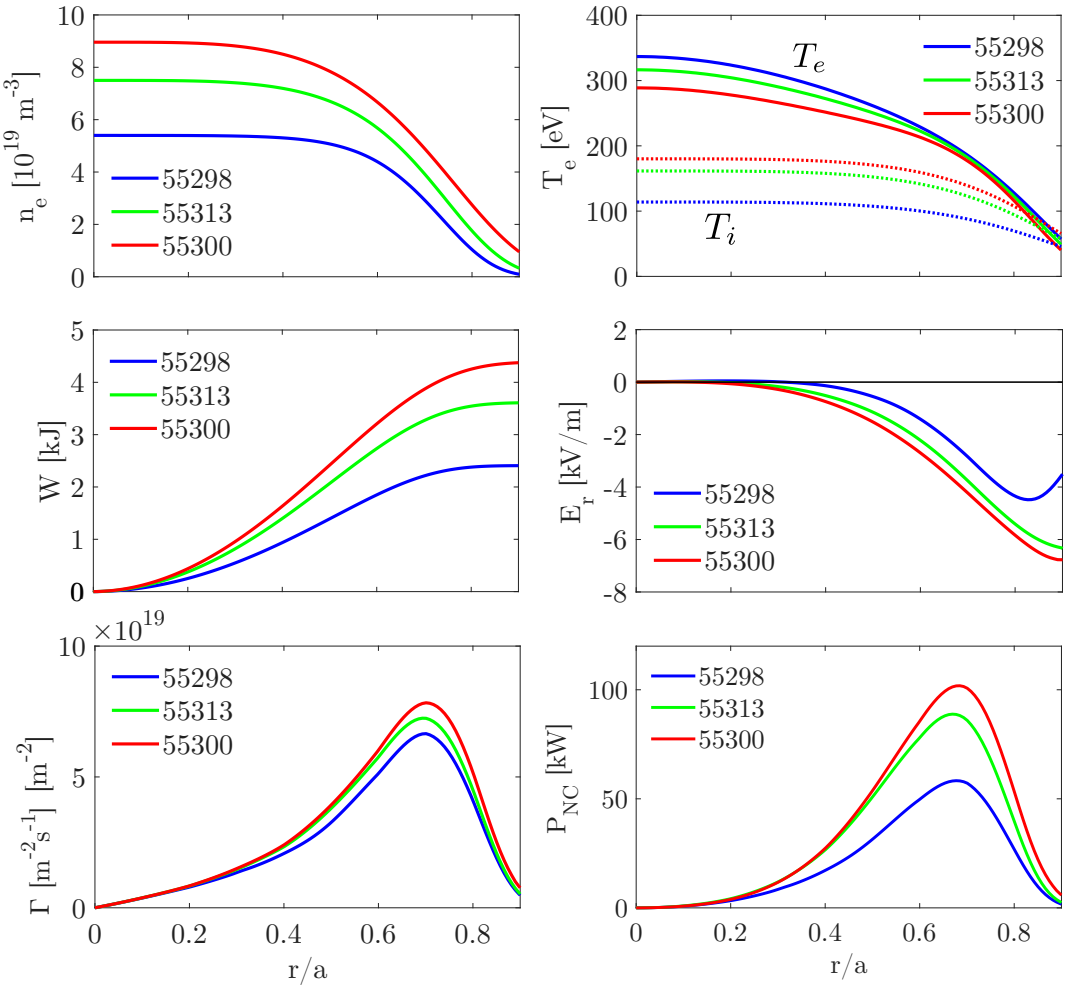

Figure 3: *From top to bottom and left to right, profiles of: electron density n_e, electron T_e (solid) and ion T_i (dotted) temperatures, integrated energy W, ambipolar radial electric field E_r, and surface integrated particle Γ and power fluxes P_{NC} for discharges #55298, #55313, and #55300.*

Under counter-NBI heating, the measured total plasma current I_p includes both bootstrap and NBI-driven components. By subtracting the neoclassical bootstrap current estimate I_b from the measured I_p of the reference discharge #55298, an NBI-driven current of $I_{NBI} \equiv I_p - I_b =$

-1.8 kA was deduced. Assuming I_{NBI} remains constant across all discharges -a significant operational assumption- this calculation yields results highly consistent with the experimentally measured current, exhibiting a discrepancy of approximately 10%.

Table 1: Comparison between experimental parameters and core neoclassical simulations.

Shot	W_{diag} [kJ]	$\tau_{\mathrm{E}}^{\mathrm{exp}}$ [ms]	$\tau_{\mathrm{E}}^{\mathrm{ISS04}}$ [ms]	$\tau_{\mathrm{E}}^{\mathrm{NC}}$ [ms]	$\tau_{\mathrm{p}}^{\mathrm{NC}}$ [ms]	I_b [kA]	I_p [kA]	$I_{\mathrm{NBI}}+I_b$ [kA]
#55298	2.4	8.2	7.5	38	50	0.3	-1.5	-1.5
#55313	3.6	11.8	10.7	35	54	0.8	-1.2	-1
#55300	4.4	13.9	12.4	36	66	1.2	-0.8	-0.6

Summary

Neoclassical simulations of the enhanced confinement regime induced by multi-pellet injection in NBI-heated TJ-II plasmas account for only a third of the global energy transport. Furthermore, contrary to experimental energy confinement scaling observations, the core neoclassical models show no confinement improvement. These findings strongly support the conclusion that the enhanced confinement regime is due to a reduction of the turbulent transport channel [9]. A systematic comparison between experimental measurements and turbulent and neoclassical simulations is currently underway to quantify the exact partition of these transport channels.

Acknowledgement

This research was partially financed by grants PID2022-137869OB-I00, PID2020-116599RB-I00 and PID2023-148697OB-I00 funded by MICIN/AEI/10.13039/501100011033, by "ERDF A way of Making Europe", and by the European Union through the Euratom Research and Training Programme (Grant Agreement No 101052200 - EUROfusion). The views and opinions expressed herein are solely those of the author(s) and do not necessarily reflect those of the European Union or the European Commission, which can hold no responsibility for them.

References

[1] I. García-Cortés *et al.*, *Phys. Plasmas* **30** 072506 (2023).

[2] K.J. McCarthy *et al.*, *Nucl. Fusion* **64** 06019 (2024).

[3] H. Thienpondt *et al.*, *Nucl. Fusion* **65** 016062 (2025).

[4] C.D. Beidler *et al.*, *Nucl. Fusion* **51** 076001 (2011).

[5] Y. Turkin *et al.*, *Phys. Plasmas* **18** 022505 (2011).

[6] V. Tribaldos *et al.*, *Phys. Plasmas* **18** 102507 (2011).

[7] S.P. Hirshman *et al.*, *Phys. Fluids* **29** 2951 (1986).

[8] H. Maaßberg *et al.*, *Phys. Plasmas* **16** 072504 (2009).

[9] I. García-Cortés *et al.*, submitted to *Nucl. Fusion* (2026).